Valuable metal recycling from thin film CIGS solar cells by leaching under mild conditions

Downloaded from: https://research.chalmers.se, 2026-04-05 13:40 UTC

Citation for the original published paper (version of record):
Teknetzi, I., Holgersson, S., Ebin, B. (2023). Valuable metal recycling from thin film CIGS solar cells by leaching under mild conditions. Solar Energy Materials and Solar Cells, 252. http://dx.doi.org/10.1016/j.solmat.2022.112178

N.B. When citing this work, cite the original published paper.

research.chalmers.se offers the possibility of retrieving research publications produced at Chalmers University of Technology. It covers all kind of research output: articles, dissertations, conference papers, reports etc. since 2004. research.chalmers.se is administrated and maintained by Chalmers Library

(article starts on next page)

Solar Energy Materials & Solar Cells 252 (2023) 112178

Contents lists available at ScienceDirect

Solar Energy Materials and Solar Cells

journal homepage: www.elsevier.com/locate/solmat

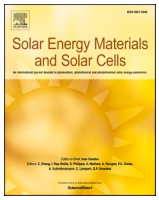

Valuable metal recycling from thin film CIGS solar cells by leaching under mild conditions

Ioanna Teknetzi *, Stellan Holgersson, Burçak Ebin

Nuclear Chemistry and Industrial Materials Recycling, Department of Chemistry and Chemical Engineering, Chalmers University of Technology, Gothenburg, SE-412 96, Sweden

ARTICLE INFO

Keywords:
Photovoltaics recycling
CIGS cell
Leaching
Metal recovery
Indium
Silver

ABSTRACT

The increase in the manufacturing of copper-indium-gallium-diselenide (CIGS) thin film photovoltaics is accompanied by a growing amount of production waste, which contains a mixture of valuable, critical and hazardous elements. However, industrial recovery and reuse processes of these elements for production of new photovoltaics are still absent. In this paper, the possibility of using benign leaching conditions for recovering mainly silver and indium from production waste flexible CIGS solar cells was investigated, along with the contamination levels from other industrial elements in the leachate. At the same time, the prospect of selective leaching of contaminants was assessed, aiming to purer streams of the valuable metals and thus their reuse in new products. The results show an increase in the leaching yields of Ag and In when acid concentration and surface to liquid ratio (A:L) increase, however, this is also true for contamination. A complete Ag recovery and 85% recovery of In was achieved with 2 M HNO_3 and A:L equal to 1:3 cm^2/ml after 24 h of leaching at room temperature. Under the same conditions, leaching with 0.5 M HNO_3 extracts 85% Ag and 30% In, with correspondingly reduced contamination levels. Finally, leaching with 0.1 M HNO_3 proved to be promising for achievement of higher Ag purity through an initial step of Zn selective leaching for 1 h.

1. Introduction

According to the International Energy Agency (IEA), photovoltaic (PV) systems accounted for 3.1% of global electricity generation in 2020, with a production of 821 TWh (23% increase compared to 2019). The "Net Zero Emissions Scenario by 2050" requires this amount to reach 6970 TWh already by 2030 [1]. Crystalline silicon based solar cells hold the largest manufacturing share, reaching 95% in 2021. The rest 5% is shared between the thin film technologies using CdTe and CIGS (Copper Indium Gallium diSelenide) as active materials [2]. There are also other technologies, like heterojunction and multi-junction/tandem solar cells, achieving high efficiencies at lab scale [2–4], increasing their market shares slowly [5]. The CIGS technology stands out for its high conversion efficiency, achieving 23.4% and 19.2% in cell and module level, respectively. The production of CIGS cells has increased and it reached 1.5 GW in 2021 [2]. In the short run, the production waste will increase with the increase of production. In the long run, the PV systems containing these cells will also need to be treated properly when they reach their end of life, after about 30 years of operation [6]. Since the CIGS technology is also a part of multijunction solar cells [7], any advances in the recycling of CIGS cells are relevant to the recycling of multijunction solar cells as well.

The CIGS cells can be rigid or flexible and are generally comprised of the following layers, from the bottom to the top: 1) a substrate made of glass, plastic or stainless steel to support the films, 2) a molybdenum back contact (0.5–2 μm), 3) the CIGS absorber layer (1–3 μm), 4) a window layer (40–80 nm) that forms the junction, usually made of CdS or other alternatives such as ZnS, ZnSe, In_2S_3, (Zn,In)Se, Zn(O,S) and MgZnO and a buffer layer (50–100 nm) made of ZnO 5) a transparent conductive oxide (TCO) layer (0.5–2 μm) made of ZnO:Al or Indium Tin Oxide (ITO) and finally 6) a conductive grid made of Ag or Al/Ni is deposited on top of the TCO for current collection [8,9]. Based on the composition of the multiple layers of these cells, the valuable and critical elements Ag, In and Ga can be present [10]. At the same time, Ag, Al, Cu, In, Mo, Ni, Zn as well as Fe and Cr (in case of stainless steel substrate), are considered hazardous for health if they contaminate the soil and/or groundwater [11–13].

A proper treatment of this waste is consequently needed because of

* Corresponding author. Nuclear Chemistry and Industrial Materials Recycling, Energy and Materials Division, Dept. of Chemistry and Chemical Engineering, Chalmers University of Technology, Kemivägen 4, SE - 41258, Gothenburg, Sweden.
E-mail address: ioanna.teknetzi@chalmers.se (I. Teknetzi).

https://doi.org/10.1016/j.solmat.2022.112178
Received 14 November 2022; Received in revised form 19 December 2022; Accepted 29 December 2022
Available online 16 January 2023
0927-0248/© 2023 The Authors. Published by Elsevier B.V. This is an open access article under the CC BY license (http://creativecommons.org/licenses/by/4.0/).

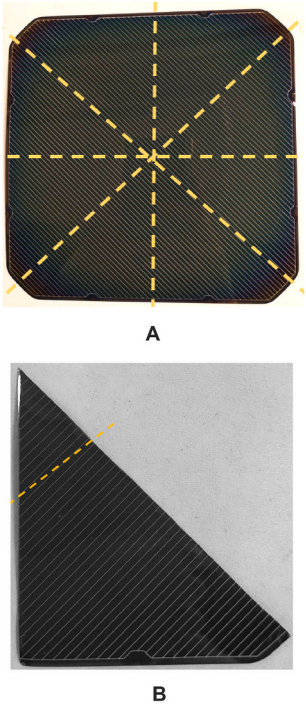

Fig. 1. a) Division of a flexible CIGS solar cell (15.6 × 15.6 cm^2) into 8 identical samples and b) the way of cutting further each sample used in the experiments.

both economical and environmental reasons: reuse of the recovered elements for the production of new solar cells could reduce their manufacturing cost, while contributing to cleaner solar energy with lower environmental footprint at the manufacturing and end-of-life stages. However, to the best of the authors' knowledge, there is no feasible industrial recycling of this waste yet. Also, the literature data on recycling of CIGS cells is very limited, with most of the relevant information coming from research on the recycling of CIGS targets and chamber waste. Some data for thermal and chemical treatment methods for the recycling of In, Ga, Se and Cu from spent CIGS targets and chamber waste are reported. Gustafsson et al. [14] suggested a thermal recycling process, starting with oxidation of the CIGS target at 800 °C to separate Se as SeO_2. For the recovery of the rest of the elements, high temperature chlorination using different chlorination agents was studied [15] and the process was finally optimized for NH_4Cl (260 and 340 °C for Ga and In recovery, respectively) [16]. Lv et al. [17] first thermally removed Se as SeO_2 and then achieved high leaching yields of In, Ga and Cu by leaching their oxides with 4 M H_2SO_4 at 90 °C. They also proved that recovery of In and Ga from the leachate is possible through their precipitation as hydroxides followed by roasting at 800 °C to obtain a mix of their oxides, while Cu can be recovered as a sulphate after solvent extraction, stripping and crystallization. On the other hand, Hu et al. [18] started with leaching a spent CIGS material using 3.2 M HNO_3 at 80 °C. Ga, Cu and some Se were present in the leachate, while In and most of Se remained in the solid residue. A precipitation step using MgO followed to recover Ga and Cu, while Se was recovered from all the solids at the end of the process through roasting at 800–900 °C. Ma et al. [19] separated Se from CIGS chamber waste as SeO_2 in a first sulphation roasting step and in a second roasting step converted the solid residue of the first step into $CuSO_4$ and oxides of In and Ga. Then Cu was removed by water leaching. In and Ga were then separated using highly concentrated (7 M) NaOH solutions. Hsiang et al. [20] used only hydrometallurgical processes for the recycling of spent CIGS targets starting with autoclave leaching with 3 M H_2SO_4 and H_2O_2 at 140 °C which dissolved Ga, In and Cu, while Se was converted into its metallic form. The dried leachate was reacted with Se powder to produce new CIGS nanoparticles. A different approach was developed by Gu et al. [21], starting with the leaching of all the elements of a spent CIGS target with 5 M HCl at 40 °C and then the separation of Cu and Se was made by electrodeposition. Dehydration of leachate with $SOCl_2$, filtration and distillation followed, in order for In and Ga to be obtained as chlorides. The information coming from these studies is valuable also for the recycling of complete CIGS cells, however, one should note that the targets and chamber waste consist only of Cu, In, Ga and Se and less contaminations of other elements. This means that high purity streams can be more difficult to obtain in the case of the recycling of whole cells, which contain more elements and therefore may show a more complicated leaching behavior. However, high purity of the recovered materials seems to be a significant factor for reducing the recycling costs [22]. Finally, Liu et al. [23] studied the recycling of real CIGS modules, starting by peeling off the active layer, but measuring only the concentration of the elements of the CIGS layer and not the contamination from elements present in other layers. Then S and Se were removed by annealing, the residue was leached with 5 M HNO_3 at 80 °C and solvent extraction with D2EHPA was used to separate In, Ga and Cu. Stripping followed and then precipitation of each metal's hydroxides. Finally, the metals oxides were recovered by calcination.

Regarding the recycling of Ag from PV, some research has been conducted with crystalline silicon PV technology instead. Many researchers have used high HNO_3 concentrations (at least 40%), as single or multi-compound solutions, and usually high temperatures as well (80 °C) [24–27]. Łażewska et al. [28], on the other hand, investigated the etching of Ag using only 1–3 M nitric acid at 30 and 50 °C. However, it is not clear what yields were achieved for each case. Another method includes the use of a sulphonic acid (RSO_3H) in the presence of H_2O_2 to dissolve Ag and then precipitate AgCl with the addition of HCl [29]. Finally, the use of other acids, like HF, CH_3COOH, H_2SO_4 and addition of H_2O_2 is vaguely described in some articles, with no more information about their proportions in case of mixtures or in general the leaching/etching conditions [30–33].

This literature review proves that leaching is in most cases an indispensable step of the recycling of solar cells materials. However, all methods described in the literature for the recovery of In, Ga, Cu and Se have used harsh leaching conditions, with high temperatures and high leaching agents' concentrations. This seems also be the case for the recovery of Ag, but specific details about the leaching conditions are also often omitted in the studies. At an industrial scale, these harsh leaching conditions are challenging both from a practical and economical perspective (corrosion, costly equipment, cost of chemicals), but also from a regulatory, safety and environmental one [34–36].

In this paper, the possibility of selective leaching and recovery of elements from flexible CIGS cells with an Ag conductive grid using nitric acid under mild leaching conditions is investigated. More specifically, this research investigates: 1) the possibility of high recovery of Ag and In (as these are considered as the most valuable elements present in the cells) and 2) suitable conditions for selective leaching of any element that can easily be removed, in order to achieve high purity streams. To maintain mild leaching conditions, nitric acid concentrations of no higher than 2 M and room temperature were used. Also, different A:L ratios were tested. The elemental composition of the leachate was determined with ICP-OES while the elemental composition of the solid residues, when necessary to determined, was performed with SEM-EDS.

2. Materials and methods

2.1. Materials

Nitric acid 69% (Suprapur, Merck) and Milli-Q water with a resistivity of 18.2 MΩ cm were used for all the leaching experiments and the ICP-OES analysis. The flexible CIGS solar cells (15.6 × 15.6 cm^2) with an Ag conductive grid and stainless steel substrate were provided by the Swedish manufacturing company Midsummer AB.

Table 1
Experiments and their conditions.

Experiment	C_{HNO3} (M)	A:L (cm^2/ml)	V_{HNO3} (ml)	T (°C)	Stirring rate (rpm)	A (cm^2)	Steps
D8M	8	1/3	90.5 ± 1.0	22 ± 1	200 ± 3	30.2	1
L0.1M-3	0.1	1/3	90.5 ± 1.0	20 ± 1	200 ± 3	30.2	1
L0.1M-5	0.1	1/5	151.0 ± 2.0	20 ± 1	200 ± 3	30.2	1
L0.1M-7	0.1	1/7	211.0 ± 2.0	20 ± 1	200 ± 3	30.2	1
L0.5M-3	0.5	1/3	90.5 ± 1.0	20 ± 1	200 ± 3	30.2	1
L0.5M-5	0.5	1/5	151.0 ± 2.0	20 ± 1	200 ± 3	30.2	1
L0.5M-7	0.5	1/7	211.0 ± 2.0	20 ± 1	200 ± 3	30.2	1
L2M-3	2	1/3	90.5 ± 1.0	20 ± 1	200 ± 3	30.2	1
L2M-5	2	1/5	151.0 ± 2.0	20 ± 1	200 ± 3	30.2	1
L2M-7	2	1/7	211.0 ± 2.0	20 ± 1	200 ± 3	30.2	1
2-L2M-3	2	1/3	90.5 ± 1.0	20 ± 1	200 ± 3	30.2	2

2.2. Experimental methods

The experiments performed in this work include a digestion of the cells at room temperature to obtain the total amount of Ag and In per cell. Then several leaching experiments at room temperature under different conditions (acid concentration, surface area to liquid ratio (A:L) and successive leaching steps) were performed to determine the yield of the leached Ag and In, as well as the levels of other contaminants. In all the experiments, the geometrical surface area to liquid ratio (A:L) is used instead of the solid to liquid ratio (S:L), since the metals of interest are present in the form of a very thin film and differences in mass from sample to sample are mainly due to differences in the mass of the stainless-steel substrate.

2.2.1. Digestion and leaching experiments

In order to use an adequate amount of sample, one cell was cut into 8 identical pieces (Fig. 1a) and then each of these samples was cut further into one small and one big piece (Fig. 1b), both used, to fit precisely in the digestion/leaching containers. For all the experiments, a sample (their masses given in the Supporting file, Table S1) was placed in a container filled with the desired volume of HNO_3 solution of a specific concentration. All the experiments were performed at room temperature and with a stirring rate of 200 ± 3 rpm. The experimental set-up consisted of a cylindrical plastic container (Ø 7.50 cm) which was kept with its cap closed during the experiment. The stirring was maintained using an automatic mechanical stirrer (RSLab-3), placed about 1 mm above the sample lying on the bottom of the container, with a hole in the cap of the container to allow the shaft of the stirrer to go through. Any spacing between the rim of the hole and the shaft was covered with parafilm and a rubber O-ring was placed on top of it to keep the parafilm in place (ie the container was not hermetically closed). This design has been proved to be very successful in reducing evaporation, with a loss of solution of only ~0.7 ml in 24 h.

Aliquots (see Supporting file material, Table S1) were taken at 1, 2, 4, 6, 8, 24, 28 and 32 h of leaching, unless otherwise is specified. The samples were then filtered with a 0.45 μm syringe filter and analyzed. After the completion of the experiments, the pieces of the solar cell were immersed in Milli-Q water for about 3 s and then removed from the water and left to air-dry. Analysis of their surface followed when considered necessary. All the experiments and their conditions are summarized in Table 1. More specifically, a complete digestion was performed with a 32 h-digestion of the solar cells with 8 M HNO_3 and A:L ratio of 1:3 cm^2/ml (experiment label D8M). Leaching experiments under mild conditions included a 32 h-leaching, using different acid concentrations (0.1, 0.5 and 2 M HNO_3) and different A:L ratios (1:3, 1:5 and 1:7) for each of the acid concentrations (experiment labels L0.1M − 7 to L2M − 3 in Table 1). A final leaching experiment was made, which examined the possibility of increasing the total leaching yields by using a 2-step leaching procedure (experiment label 2-L2M − 3). In that experiment, the sample was first leached with 2 M HNO_3 and with A:L equal to 1:3 for 24 h and then the sample was removed and placed in another container with fresh/pure solution of the same specifications for another 24 h of leaching.

All experiments were made in replicates of three. The three samples for each triplicate were taken from different cells. The error calculated and presented in all tables and plots along with the results is the standard deviation of the respective triplicate.

2.2.2. Analysis and instrumentation

The elemental analyses of the leaching aliquots were performed with Inductively Coupled Plasma – Optical Emission Spectroscopy (ICP-OES, ThermoScientific iCAP PRO), using elemental standards (1000 ppm, Inorganic Ventures). For the surface morphological study and qualitative (due to the inherent heterogeneity of samples) elemental analysis of the solid samples, Scanning Electron Microscopy coupled with Energy Dispersive X-ray Spectroscopy (SEM-EDS, FEI Quanta 200 FEG SEM with an Oxford Instruments X-Max EDS detector) was used.

2.2.3. Calculation of leaching yield

For all elements, the leached mass of each element per cell [mg/cell] after *t* hours of leaching is calculated based on the formula:

$$mass/_{cell} = C_{ICP} \bullet DF \bullet V_{solution} \bullet 8 \quad (1)$$

where C_{ICP} is the concentration measured with the ICP [ppm or mg/l], DF the dilution factor of the sample measured with the ICP, $V_{solution}$ the volume of the solution [ml] at the time of the sampling and the factor 8 is because each sample is the 1/8 of the whole cell.

Based on the area of each sample, 30.2 cm^2, the leached mass of each element per area of the cell [μg/cm^2] is calculated as:

$$mass/_{area} = 1000 \bullet C_{ICP} \bullet DF \bullet V_{solution} \Big/ 30.2 \quad (2)$$

Finally, for the calculation of the yields for Ag and In the following formula is used:

$$\%\ Yield = 100 \bullet \frac{mass/_{cell}}{(mass/_{cell})_{total}} \quad (3)$$

where $(mass/cell)_{total}$ is the total mass of the element, determined by the digestion experiments D8M.

3. Results and discussion

3.1. Thermodynamic investigation of possible reactions for the main elements

The HSC Chemistry 10 software was used for thermodynamic data acquisition and evaluation of the reactions that can take place. A list of the possible reactions between the main elements that are present in the CIGS cell and nitric acid are given in Table S2 along with the values of their standard enthalpy (ΔH°), entropy (ΔS°), Gibbs free energy (ΔG°) and equilibrium constant (K). According to thermodynamics, a reaction is spontaneous when its Gibbs free energy (ΔG) is negative. At equilibrium, ΔG° and K are related with the following relation:

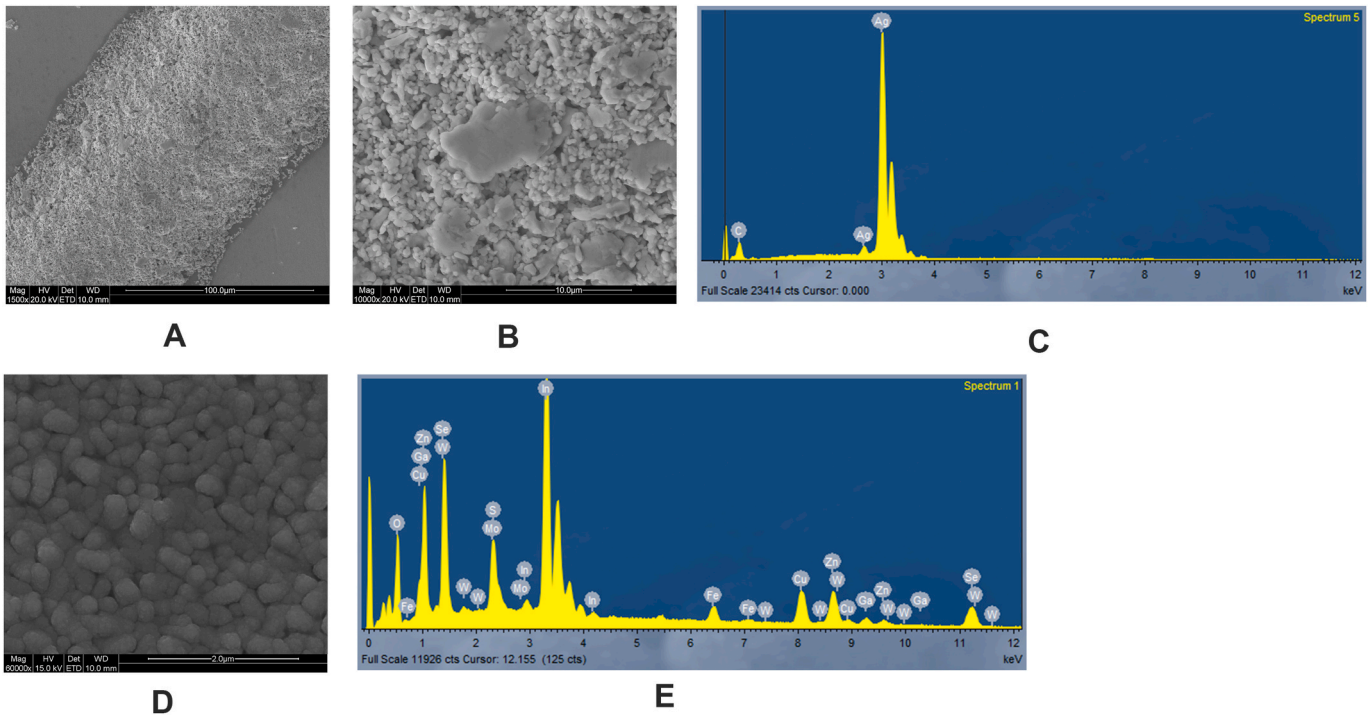

Fig. 2. Morphological and elemental analysis of the original sample. a), b) SEM images of the Ag conductive grid taken with secondary electrons at magnifications of×1500 and ×20 k, respectively, c) the EDS spectrum of (b), d) SEM image of the top layer of the CIGS solar cell taken with secondary electrons at a magnification of x60 k and e) its respective EDS spectrum.

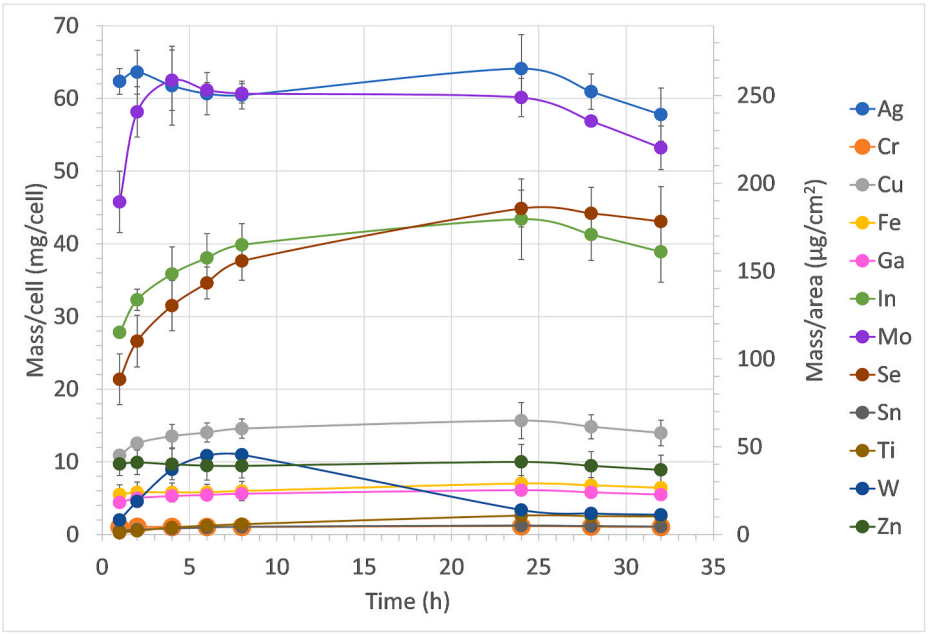

Fig. 3. Plot of mass of element per cell and per area vs time of the digestion of solar cells with 8 M HNO_3 and A/L equal to 1/3 (experiment D8M).

$$\Delta G^{\circ} = -RT\ln K \quad (4)$$

When not at equilibrium, ΔG, ΔG° and the reaction quotient (Q) are related to each other with eq. (5):

$$\Delta G = \Delta G^{\circ} + RT\ln Q \quad (5)$$

Regarding the reactions between the CIGS layer and nitric acid, since the whole CIGS compound is not available in the HSC database, the simple selenides from which it forms (Cu_2Se, In_2Se_3 and Ga_2Se_3) were considered. Based on their standard Gibbs free energies (ΔG°) and equilibrium constants (K), their redox reactions (Table S2 Eqs. 4-27) are expected to be spontaneous, but this is not the case for the double replacement reactions (Table S2 Eqs. 1–3). In short, the selenides should react with HNO_3 and produce the respective metal nitrates, water, NO and/or NO_2 and Se, SeO_2(g), SeO_2(s) and/or SeO_2(aq). At the same time, the formation of the water soluble selenious acid H_2SeO_3 [37] through the reaction of SeO_2 with water is also likely to be thermodynamically favored (Table S2 Eqs. 28, 29 and 31).

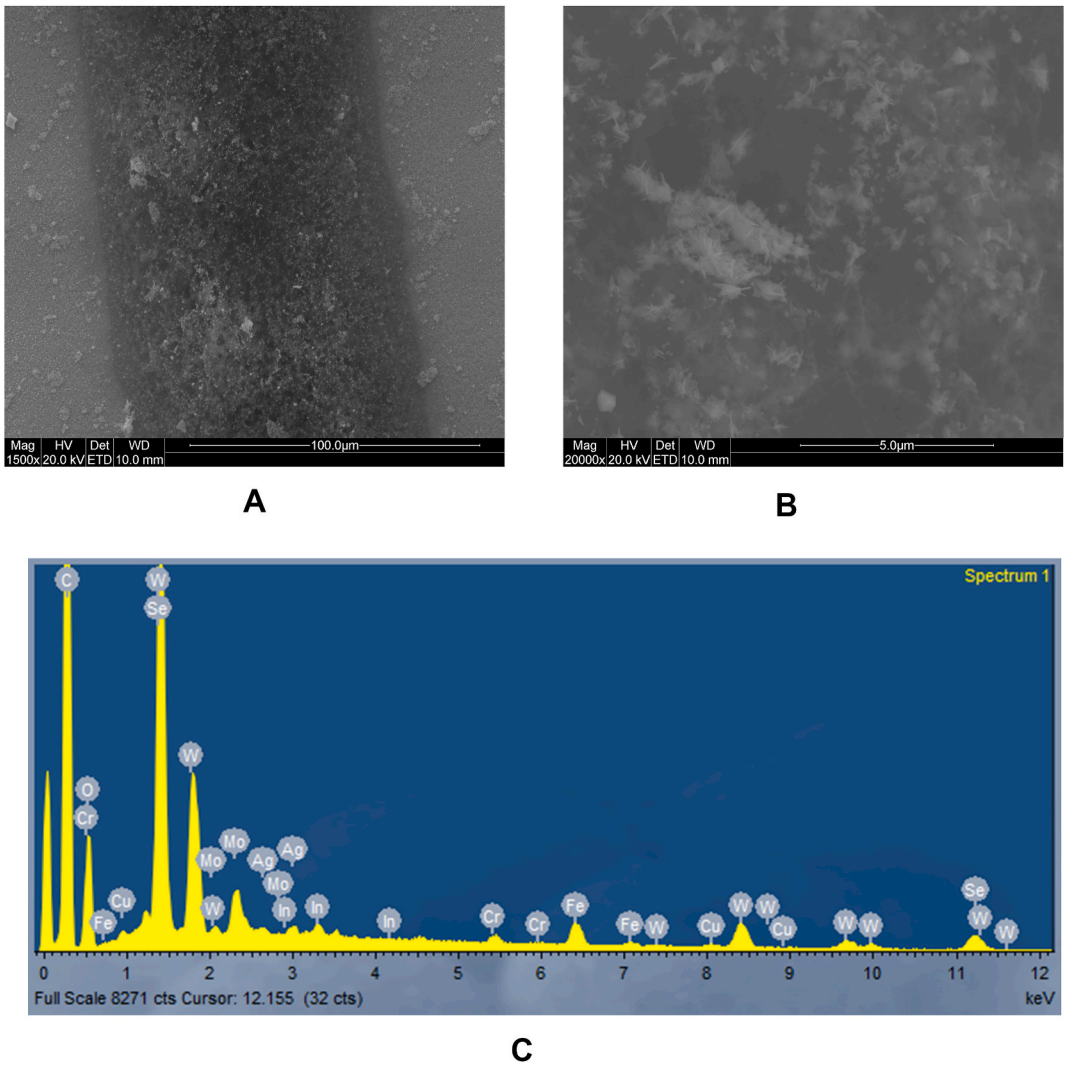

Fig. 4. Morphological and elemental analysis of the 32 h-digested sample. a), b) SEM images of the Ag conductive grid taken with secondary electrons at magnifications of×1500 and ×20 k, respectively, c) the EDS spectrum of (b), d) SEM image of the top layer of the CIGS solar cell (area 1) and a layer underneath (area 2) taken with secondary electrons at a magnification of x20 k and e, f) the EDS spectra of points 1 and 2 of (d), respectively.

Ag and Mo are present in the cells in their metallic form. Possible Ag reactions with nitric acid are suggested in Table S2 Eqs. 36–38 and form its nitrate, water and H_2, NO and/or NO_2. Based on their ΔG° and K values, only the reactions forming NO_x can be spontaneous, as expected. In the case of Mo, the formation of molybdic acid, $MoO_3 \bullet H_2O$, seems thermodynamically favored to take place (Table S2 Eqs. 39–40). Other species of Mo that can be present are MoO_3(aq) and $MoO_3 \bullet 2H_2O$ [38]. For constant temperature, the solubility of all those Mo compounds depends on the nitric acid concentration [38].

Regarding Fe and Cr coming from the stainless-steel substrate, it is well known in the steel industry that nitric acid is used for passivation of the stainless steel through a creation of a chromium oxide layer, with some Fe also being removed from the surface during this process. The passivation treatment in the industry is quick and does not take more than 1 h, while the temperature needed can even be as low as room temperature [39]. Therefore, these reactions are expected to take place on the stainless steel substrate of the CIGS cells for the experimental conditions of this study.

In summary, the thermodynamic analysis suggested that leaching of the metals found in the CIGS layer and the Ag grid with HNO_3 is possible through redox reactions. At the same time, Se can form various products, in aqueous, solid or gaseous phase which can form selenious acid after reacting with water. Regarding Mo, molybdic acid can form as well as other, partly soluble, oxides. Finally, contamination from the stainless steel substrate was expected to be limited, due to its passivation by the nitric acid.

3.2. Morphological and elemental analysis of the original samples

The SEM-EDS analysis of the original cells confirmed the presence of Ag particles in the conductive grid (Fig. 2c) and revealed that they have a wide size distribution, ranging from less than 1 to more than 10 µm (Fig. 2a and b). Regarding, the presence of carbon in the EDS spectrum (Fig. 2c), it is known from the manufacturer that the Ag grid is created by using a silver paste, therefore C is assigned to the residual organic compounds of this paste.

Regarding the morphology of the top layer, it has a nodular homogeneous structure, as shown in Fig. 2d. An EDS analysis reveals the presence of multiple elements: Zn, S, Cu, In, Ga, Se, Mo, W and Fe (Fig. 2e). Fe is normally not an element that is used for the manufacturing of any of the layers and therefore it can be said with certainty that its signal comes from the underlying stainless-steel substrate. This means that the penetration depth of the electron beam is larger than the total thickness of all the film layers together and the

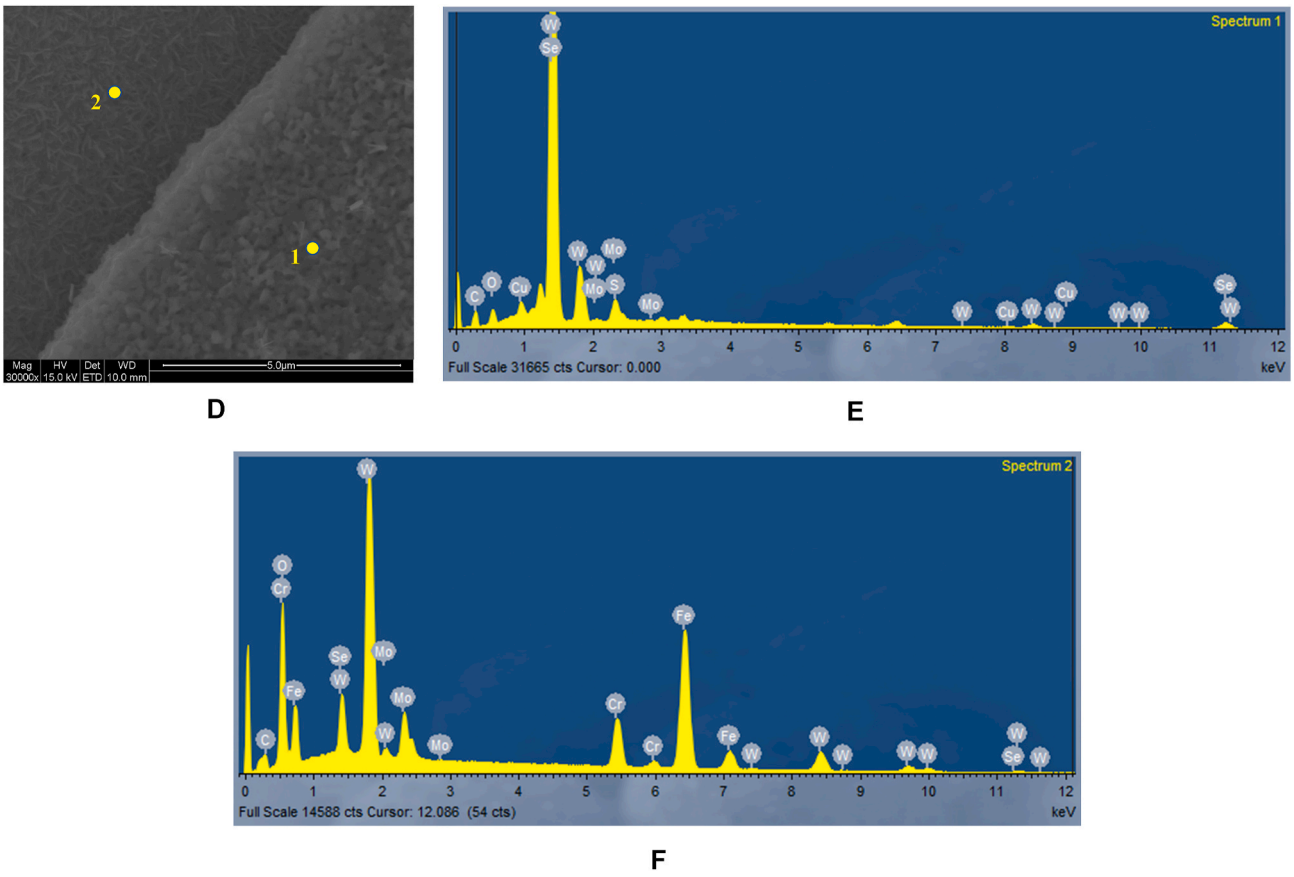

Fig. 4. (*continued*).

beam collects information from all of them, until it reaches the substrate. This is in agreement with the theory of the interaction volume of the electron beam, which can exceed the 1 μm in depth and width, depending on the acceleration voltage and the density of the material [40], and the thickness of the film layers. Therefore, with this method the morphology and chemical composition observed cannot be assigned with certainty to any specific layer.

3.3. Total mass of Ag and In per cell

The results of the digestion of the cells experiment (Experiment D8M) are presented in Fig. 3 and are given both in mass of element per cell (mg/cell) and also in mass per area of the cell (μg/cm^2). According to these results, the maximum yield for all the elements is achieved after 24 h of digestion under the experimental conditions. The only exception is W, which reaches its maximum value after 6 h and then starts precipitating (Fig. 3). The total mass of Ag and In are 64.1 ± 4.7 mg/cell and 43.4 ± 5.5 mg/cell, respectively.

To verify that the leached amounts of Ag and In given in Fig. 3 are also the total amounts of these elements per cell, the residues on the surface of the cell samples after 32 h of digestion were analyzed with SEM-EDS (Fig. 4). It is evident that the Ag conductive lines have practically disappeared, leaving only the organic compound behind (as the dark tone of the grid line indicates in Fig. 4a–b), along with some precipitates of other elements. The analysis of the top layer (Fig. 4d–f) confirms that all the In has practically been dissolved, as well.

It is worth mentioning that Cu, Se, W and Mo (detected with EDS in Fig. 4c, e and f) only dissolved partly under these experimental conditions. Regarding Se, the EDS analysis detected a strong peak at 1.4 keV in the top layer, as shown in Fig. 4e, which is assigned mainly to Se and not to W, since the strongest peak of W is at about 1.8 keV. The absence of strong oxygen peak in the spectrum of Fig. 4e suggests that the remaining Se anion of the diselenide compound in the digestion residue may have mainly oxidized to its elemental form. A small peak of Cu is also detected in the same spectrum. A remaining Cu-and-Se-rich CIGS layer and/or a reaction between Cu and some of the Se towards formation of the difficult to dissolve CuSe and $CuSe_2$ is possible, as it has been observed by Hsiang et al. [20] during microwave digestion of CIGS targets with H_2SO_4 and H_2O_2. W and Mo are mainly detected in a layer underneath (Fig. 4d and f, area 2) and are expected to be in the form of their respective acids and/or oxides, as these reactions are thermodynamically favored (Table S2 Eqs. 39–42) and the precipitation of W observed in Fig. 3 is in agreement with the precipitation of tungstic acid, H_2WO_4, observed by Lee et al. [41] upon the reaction of tungsten carbide with aqua regia. A complete dissolution of Ag and In were nevertheless achieved, which was the main purpose of the digestion.

3.4. Leaching results

3.4.1. Single step leaching experiments

The scope of testing a concentration of HNO_3 as low as 0.1 M was mainly to investigate the possibility of selective leaching of elements other than Ag, since Ag as a noble metal was not expected to be affected by such dilute concentration of acid. The results of all the leaching experiments performed with 0.1 M HNO_3 and A:L ratios of 1:3, 1:5 and 1:7, (experiments L0.1M-3,5,7) are presented in Fig. 5, both in mass of element per cell (mg/cell) and also in mass of element per area of the cell (μg/cm^2). The relative standard deviations are given in Table S3, while the %yields for Ag and In for each of these leaching experiments and for every sampling time point are summarized in Table 2.

The first immediate observation is that the leaching efficiency of all the elements is practically independent of the A:L studied when 0.1 M

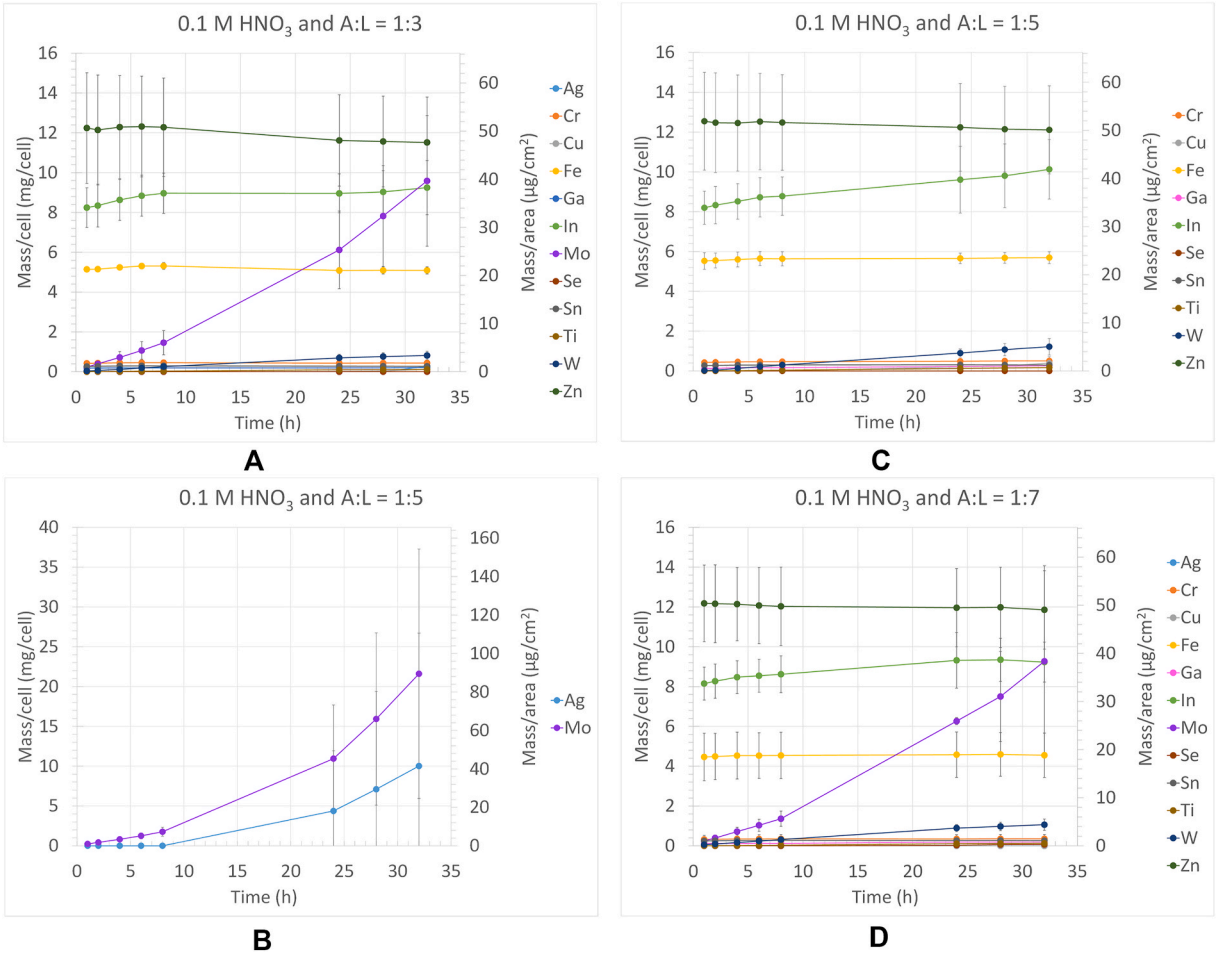

Fig. 5. Plots of mass of element per cell and per area vs time (a, c for major elements and b, d for minor) for leaching with 0.1 M HNO_3 and A:L ratios a) 1:3, b-c) 1:5 and d) 1:7 (experiments L0.1M − 3, L0.1M − 5 and L0.1M − 7, respectively).

Table 2
% Leaching yields of Ag and In for the leaching experiments with 0.1 M HNO_3 and A:L ratios of 1:3, 1:5 and 1:7, respectively.

Time (h)	L0.1M-3		L0.1M-5		L0.1M-7	
	Ag (%)	In (%)	Ag (%)	In (%)	Ag (%)	In (%)
1	n.d.	19 ± 5	n.d.	19 ± 4	n.d.	19 ± 4
2	n.d.	19 ± 5	n.d.	19 ± 5	n.d.	19 ± 4
4	n.d.	20 ± 5	n.d.	20 ± 5	n.d.	20 ± 4
6	n.d.	20 ± 5	n.d.	20 ± 5	n.d.	20 ± 4
8	n.d.	21 ± 5	n.d.	20 ± 5	n.d.	20 ± 5
24	n.d.	21 ± 5	7 + 12 - 7	22 ± 7	n.d.	21 ± 6
28	n.d.	21 ± 5	11 + 20 - 11	23 ± 7	n.d.	22 ± 5
32	n.d.	21 ± 6	16 + 27 - 16	23 ± 6	n.d.	21 ± 5

n.d.: not detected.

HNO_3 is used. Also, Ag practically is not extracted with such low acid concentrations, as expected. However, about 20% of In is recovered within the first 1 h and the leaching yield practically remains constant afterwards. A possible explanation is that In is also present in layers other than the absorber (i.e. in the TCO and/or window layers), which are the first to be exposed to the acid. Zn can be fully recovered within the first 1 h, at a yield of 12 ± 2 mg/cell for all the A:L studied. The complete and quick dissolution of Zn even in the case of a weak acidic solution can also be attributed to the fact that Zn can be found in the layers closer to the exposed surface of the cell (buffer and/or window layer), as well as the possible high solubility of the Zn compounds. Some contamination of Fe of about 5 mg/cell is also detected and remains constant with time, as expected (passivation), while the same trend is observed for Cr at 0.5 mg/cell. Finally, some Mo is also leached, starting to dissolve after 1 h and then increasing in concentration with time. After 32 h of leaching with A:L ratios 1:3 and 1:7, Mo concentration is about 10 ± 4 mg/cell. In the case where A:L ratio is 1:5, the yield ranges from 6 to 35 mg/cell after 32 h of leaching. All the other elements are only present as a very low contamination of no more than 1 mg/cell, even after 32 h of leaching for any A:L ratio tested.

The results of the leaching experiments performed with 0.5 M HNO_3 and A:L equal to 1:3, 1:5 and 1:7 (experiments L0.5M-3,5,7) are presented in Fig. 6, both in mass of element per cell (mg/cell) and also in mass of element per area of the cell (μg/cm^2). The relative standard deviations are given in Table S3, while the yields for Ag and In for each of these leaching experiments and for every sampling time point are summarized in Table 3.

Regarding Ag, its leaching is negligible for the first 8 h for all the A:L ratios studied. After 24 h the Ag yield is 88 ± 24%, 77 ± 7% and 68 ± 21% for A:L ratios of 1:3, 1:5 and 1:7, respectively, and remains practically stable after this time. One should note that the total yield of Ag extraction seems to increase with the increase of the A:L ratio. Regarding In, about 20% of total amount present has been leached after 1 h for all the A:L ratios tested and then the yield increases only slowly with time, to reach approximately 30–35% after 32 h of leaching. The fact that leaching of In starts again from 20%, as it was the case for 0.1 M HNO_3, confirms the assumption that some In should also be present in the layers

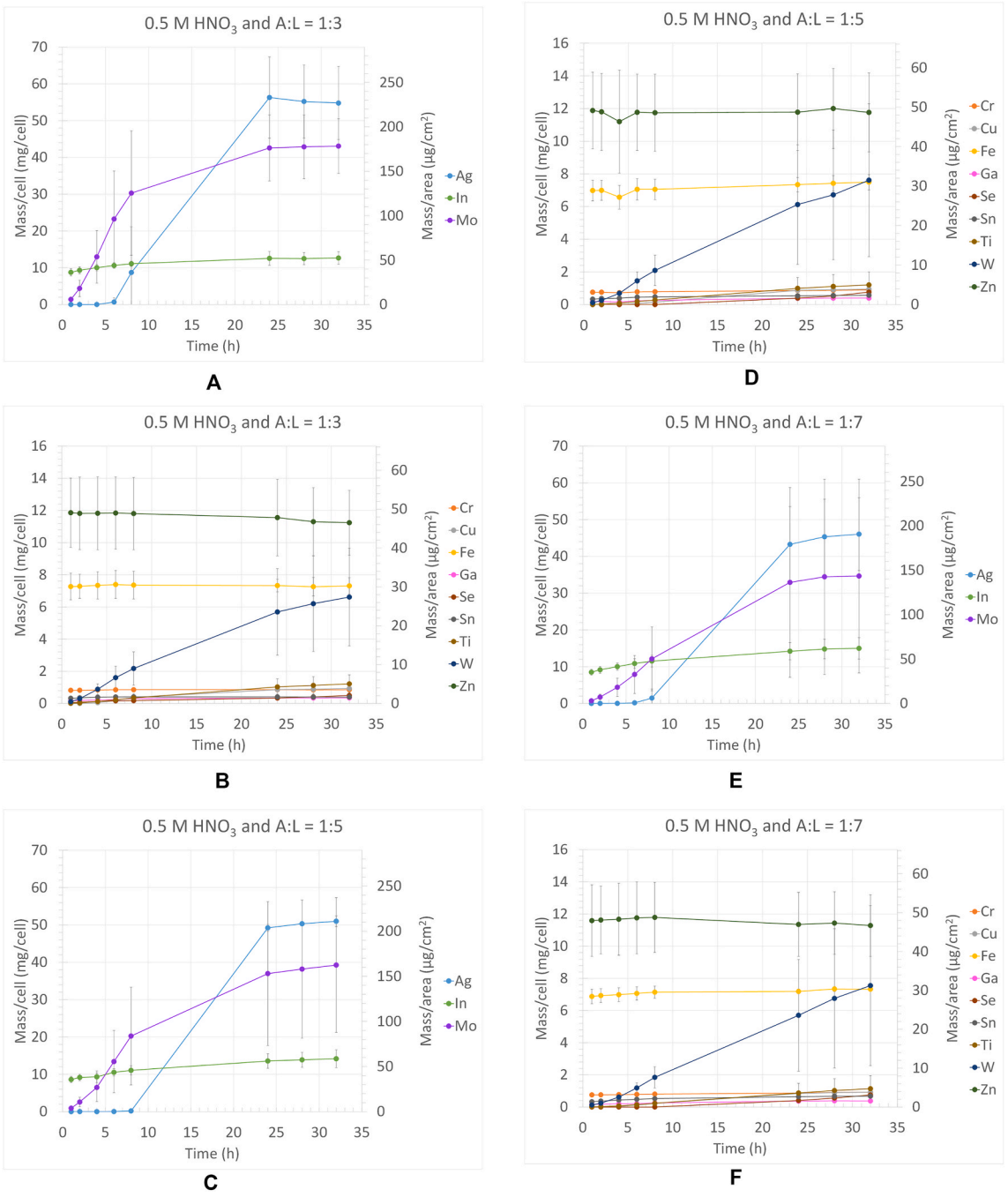

Fig. 6. Plots of mass of element per cell and per area vs time (a, c, e for major elements and b, d, f for minor) for leaching with 0.5 M HNO_3 and A:L equal to a-b) 1:3, c-d) 1:5 and e-f) 1:7 (experiments L0.5M − 3, L0.5M − 5 and L0.5M − 7, respectively).

above the CIGS layer.

For Zn, a complete dissolution has been achieved from the first hour of leaching and its concentration remains constant at 12 ± 2 mg/cell during the 32 h. Mo starts to be leached after the first hour of leaching for all the A:L ratios tested and then an increase in its leaching rate is observed as A:L ratio increases. After 32 h of leaching, the yield of Mo is about 43 ± 7, 40 ± 18 and 35 ± 26 mg/cell for A:L ratios of 1:3, 1:5 and 1:7, respectively. The quick leaching of Mo (Fig. 6) makes its complete separation from Ag by selective leaching out of question for 0.5 HNO_3 solution. However, almost 70% of the leachable Mo can still be removed from the cells within 6 h of leaching, without any significant loss of Ag. By applying such a leaching step first, purer Ag leachate can be obtained later in a second leaching step. The leaching of all other elements is not affected by the A:L ratios studied: W dissolution starts after about 2 h of leaching and increases almost linearly with time, to reach about 7 ± 3 mg/cell at 32 h, Fe and Cr amounts in the leachate remain constant during the 32 h of leaching, reaching about 7 ± 1 mg/cell and 1 mg/cell, respectively, while for the rest of the elements (Cu, Ga, Se, Sn and Ti) a maximum of 1–2 mg/cell of each is leached during the 32 h.

The results of the leaching experiments performed with 2 M HNO_3 and A:L ratios of 1:3, 1:5 and 1:7 (experiments L2M-3,5,7) are presented in Fig. 7, both in mass of element per cell (mg/cell) and also in mass of element per area of the cell (µg/cm^2). The relative standard deviations are given in Table S3, while the yields of Ag and In for each of these leaching experiments and for every sampling time point are summarized in Table 4.

Table 3
% Leaching yields of Ag and In for the leaching experiments with 0.5 M HNO_3 and A:L equal to 1:3, 1:5 and 1:7.

Time (h)	L0.5M-3		L0.5M-5		L0.5M-7	
	Ag (%)	In (%)	Ag (%)	In (%)	Ag (%)	In (%)
1	n.d.	20 ± 5	n.d.	20 ± 4	n.d.	20 ± 4
2	n.d.	21 ± 5	n.d.	21 ± 5	n.d.	21 ± 5
4	n.d.	23 ± 5	n.d.	21 ± 6	n.d.	23 ± 5
6	1 + 2 - 1	24 ± 5	n.d.	24 ± 5	n.d.	25 ± 6
8	14 + 20 - 14	26 ± 5	n.d.	25 ± 6	2 ± 4	27 ± 7
24	88 + 12 - 24	29 ± 8	77 ± 7	31 ± 9	68 ± 21	33 ± 10
28	86 + 14 - 22	29 ± 8	79 ± 6	32 ± 9	71 ± 21	34 ± 10
32	86 + 14 - 22	29 ± 8	80 ± 8	33 ± 10	72 ± 21	35 ± 11

n.d.: not detected.

A high recovery rate is achieved for Ag when 2 M HNO_3 and A:L ratio of 1:3 are used, with about 90% of total Ag being recovered between 4 and 6 h, while after 24 h the dissolution of Ag is complete. For the cases of A:L ratios of 1:5 and 1:7, the corresponding maximum yields achieved are 74 ± 25% and 80 ± 19%, respectively. Regarding In, 20–25% of total In is recovered within the first hour of leaching, while the highest yields of 85 ± 20%, 55 ± 18% and 42 ± 7% for A:L ratios of 1:3, 1:5 and 1:7, respectively, are achieved after 28 h. Some amount of Mo is leached already after 1 h and Mo shows a high dissolution rate under all the experimental conditions for at least the first 6 h. After 28 h of leaching, Mo recovery reaches a plateau, with the recovered masses being about 59 ± 9, 50 ± 5 and 42 ± 14 mg/cell for A:L ratios of 1:3, 1:5 and 1:7, respectively. A considerable amount of Se can be leached with 2 M HNO_3 and A:L ratio of 1:3, starting after 2 h of leaching and reaching a plateau at 32 ± 6 mg/cell after 24 h. For the smaller A:L ratios, the leaching of Se starts also after 2 h but reaches only 9 ± 5 and 5 ± 2 mg/cell for the 1:5 and 1:7 A:L ratios, respectively. Cu starts dissolving after 1 h of leaching and a considerable amount of 11 ± 2 mg/cell can be recovered after 28 h of leaching for A:L ratio of 1:3. For the lower ratios, lower recovery is achieved, of about 3 ± 2 and 1.5 ± 0.5 mg/cell for the 1:5 and 1:7 A:L ratios, respectively. For W the recovery is of about 10, 1 and 1 mg/cell for the 1:3, 1:5 and 1:7 A:L ratios, respectively. Some Ga is also leached, reaching about 3, 1 and 1 mg/cell at 28 h for the respective A:L ratios. Regarding Ti, a small amount is also leached with time and reaches about 2–3 mg/cell after 32 h, for all the three A:L ratios.

Finally, the recoveries of the elements Zn, Sn, Fe and Cr are rapid and then remain relatively stable with time. For Zn it is close to 9–10 mg/cell and for Sn to 1 mg/cell, for all the three A:L ratios tested. The amount of Cr leached when A:L equals 1:3 and 1:5 is 2 mg/cell, while for A:L equal to 1:7 is 1 mg/cell. Regarding Fe, A:L equal to 1:3 and 1:5 results in 12 mg/cell and A:L equal to 1:7 yields 7 mg/cell.

When comparing all the results for the different experimental conditions it can be said that the high yields of Ag and In are always accompanied by high contamination levels from many other elements, with Zn being always present. Contamination with Mo can also be a problem. This means that selective leaching is necessary if purer streams are decided to be obtained. Another observation is that an increase in acid concentration for the same A:L can generally achieve higher yields for almost all the elements, except Zn, and/or increase their leaching rate, as expected. Increase of A:L ratio seems to increase yields for most elements, but only for the two highest acid strengths. Zn, on the other hand, seems to be almost instantly released, irrespective of conditions. A comprehensive comparison of the recovery of each element after 24 h under all the different leaching conditions tested is given in the form of 3D and their respective contour plots in the Supporting file Fig. S1 and S2. These plots show clearly the increased contamination levels for the conditions where high Ag and In leaching efficiency were observed.

An increased leaching of some of the elements with increasing the A:L ratio (ie with the decrease in solution volumes) was somewhat unexpected since the available area is held constant. The opposite trend is usually observed due to an expected onset of depletion of leachant and/or a build-up of reaction products in the case of diffusion-limited leaching [42]. In our case, the build-up of counter-ions may instead assist further leaching of metals. Another explanation may be that in the case of low liquid volumes, a better in-mixing of oxygen from air can be the case. The addition of oxygen in leaching system can increase the leaching rates and yields, since oxygen is an additional oxidizing agent [43]. The only element which doesn't follow this trend is W, which for the case of 2 M HNO_3 showed a decrease in its yield with the increase of A:L ratio. However, taking into account the precipitation of W when the cells were digested with 8 M HNO_3 due to its oxidation to its acid form, the lower concentration of W in the leachate of A:L of 1:3 indicates also more oxidizing conditions. This supports the scenario of better oxygenation of the solution when low volumes are used.

It is also important to point out that the presence of Sn is confirmed with the ICP analysis of total metal content (Fig. 3), indicating the presence of ITO (a mixed oxide of In_2O_3 and SnO_2) as the TCO layer. The low amount of Sn (no more than 1 mg/cell) is consistent with that Sn was not detected with EDS (Fig. 2e). Also, SnO_2 dissolution in nitric acid can be challenging, as shown from the positive values of the ΔG of all the possible reactions of it with nitric acid (Table S2 Eqs. 47–51) and from the literature [44]. Another important observation is that the yield of In is always close to 20–25% for the first hour of leaching, with no other element from the CIGS layer being leached at this stage, implying that a constant amount of In should have been leached first from a layer(s) above CIGS. The ΔG values of the possible reactions of In_2O_3 with nitric acid (Table S2 Eqs. 43–46) suggest that they can react towards formation of indium nitrate, water and/or indium hydroxide. The formation of NO and O_2 is also likely. It has also been proved experimentally from other researchers that leaching of In from ITO using HNO_3 is possible [44–46].

Another interesting point, for all the experimental conditions tested, is that there is a general trend for Mo, W and all elements contained in the CIGS layer to start leaching first after 1 h or to have very low concentrations in the leachate if they are present before this stage. This could be at least partly attributed to the relative position of the various layers in the cell: leaching starts from the top layers, since these are the ones that they come in contact with the acid first, and only after they start dissolving the acid will reach the CIGS layer and the ones underneath, which are closer to the bottom of the cell. However, a perfect layer-by-layer leaching is impossible in the presented experimental set-up design because of the friction and mechanical impact of the mechanical stirrer on the cell.

In summary, the one-stage leaching results showed that a complete recovery of Ag can be achieved with 2 M HNO_3 and A:L ratio of 1:3, after about 24 h of leaching. The same conditions have also achieved the highest yield for In; about 85 ± 20%. However, at the same time, the contamination levels from all the other elements are also considerable. If the leaching of contaminant elements could be delayed relative to Ag and In, or vice versa, a separation would have been possible. However, this is not the case under the studied experimental conditions. Notably, Mo has shown in many cases similar leaching concentrations with the ones of Ag. To obtain purer leachates of Ag with minimized contamination, an alternative selective leaching approach is needed. Considering this concept, promising results are also obtained using 0.5 M HNO_3 and A:L ratio of 1:3, since the recovery rate of Ag reaches about 85% after 24 h and the contamination levels from other elements are lower compared to the case of 2 M acid. However, the recovery of In is also low, about 30%. Regarding selective leaching, a promising approach is the removal of Zn first, during a leaching step using 0.1 M HNO_3, which can be as fast as less than 1 h. In this step, an amount of contamination coming from Fe and Cr can also be removed along with Zn. The contamination levels of Mo in the Ag containing leachate can also be reduced if 0.5 M HNO_3 and A:L ratio of 1:3 is performed for 6 h,

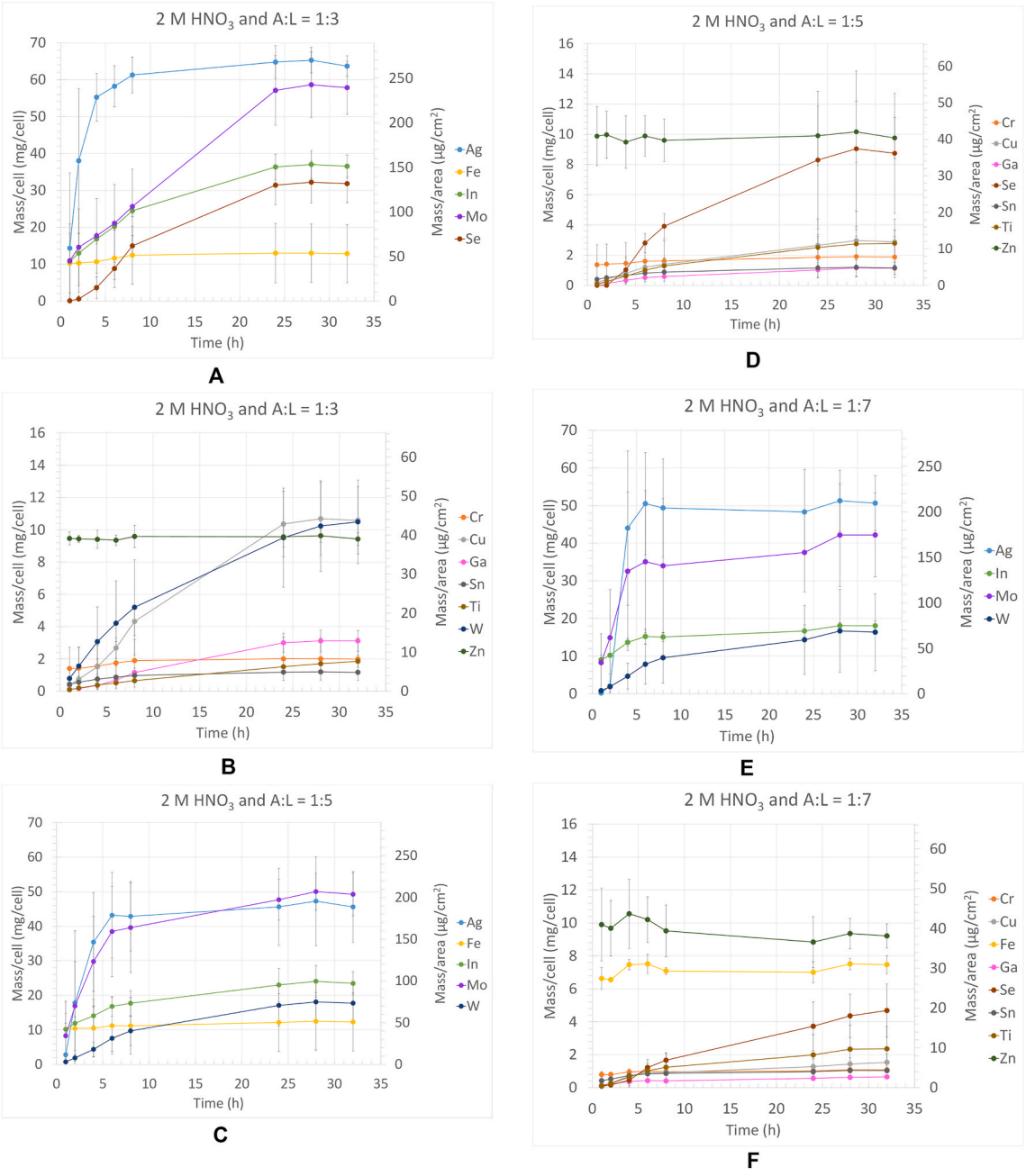

Fig. 7. Plots of mass of element per cell and mass per area vs time (a, c, e for major elements and b, d, f for minor) for leaching with 2 M HNO_3 and A:L equal to a-b) 1:3, c-d) 1:5 and e-f) 1:7 (experiments L2M − 3, L2M − 5 and L2M − 7, respectively).

however, some quantity of Ag is also possible to end up in this stream and further optimization is needed.

Finally, it is important to point out here that the total dissolution of Ag and In in the leachate means concentrations of ~90 ppm and ~60 ppm, respectively, for A:L ratio of 1:3. This shows that even if leaching achieves a 100% yield, the concentrations of the elements are still too low to be used directly in a feasible purification process which usually demands more than 1 g/l [28]. Some means to up-concentrating, for example by a reuse of the same leachate for multiple cells, should be considered for industrialization. A few examples of elements that could be recovered from the leachate after the achievement of the desired concentration, is In, Ga and Cu by means of solvent extraction [23], Ag by electrowinning [47], Mo and W possibly by precipitation due to their tendency to form oxides with limited solubility (see 3.1) etc.

3.4.2. *Results for two successive leaching steps*

According to the previously discussed leaching experiments, after 24 h of leaching using 2 M HNO_3 and A:L ratio of 1:3 (experiment label 2-L2M − 3), Ag has been completely extracted from the CIGS cells, however the recovery of In has reached a plateau at about 85%. Therefore, a successive leaching step under the same conditions was tested as a possible way to assist a complete recovery of In. The results of the second leaching step are presented in Fig. 8, both in mass of element per cell (mg/cell) and also in mass of element per area of the cell (μg/cm^2). Fig. 8 reveals that a successive second leaching step under the same conditions is ineffective for dissolving further a considerable amount of In, since the yield is only about 1% after 24 h. It is also worth noticing that the situation is similar for all the elements except W.

Table 4
% Leaching yields of Ag and In for the leaching experiments with 2 M HNO_3 and A:L equal to 1:3, 1:5 and 1:7.

Time (h)	L2M-3		L2M-5		L2M-7	
	Ag (%)	In (%)	Ag (%)	In (%)	Ag (%)	In (%)
1	22 + 33 - 22	25 ± 4	4 + 10 - 4	23 ± 7	n.d.	21 ± 6
2	59 ± 35	30 ± 5	28 + 35 - 28	27 ± 8	3 ± 5	24 ± 4
4	86 + 14 - 16	39 ± 8	55 ± 26	32 ± 11	69 ± 37	32 ± 7
6	91 + 9 - 15	47 ± 8	67 ± 24	39 ± 11	79 + 21 - 27	35 ± 9
8	96 + 14 - 15	56 ± 11	67 ± 21	41 ± 14	77 + 23 - 26	35 ± 7
24	100	84 + 16 - 19	71 ± 23	53 ± 18	75 ± 23	38 ± 9
28	100	85 + 15 - 20	74 ± 25	55 ± 18	80 ± 19	42 ± 7
32	100	84 + 16 - 18	71 ± 21	54 ± 15	79 ± 17	42 ± 8

n.d.: not detected.

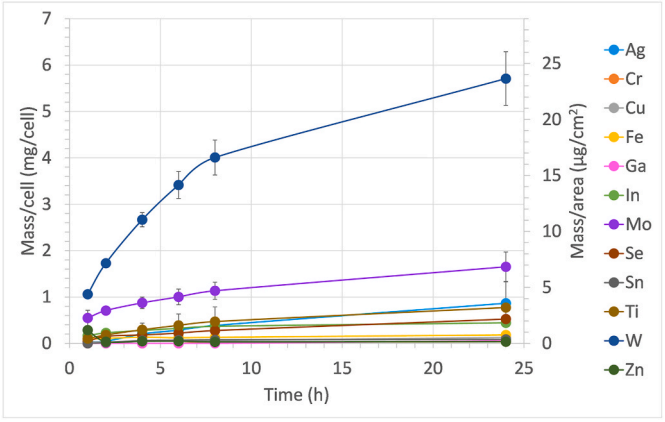

Fig. 8. Plot of mass of element per cell and per area vs time for leaching with 2 M HNO_3 and A:L ratio equal to 1:3 of the second successive leaching step (experiment 2-L2M − 3).

3.4.3. Sources of observed errors

In the majority of leaching plots, considerably high standard deviations of the triplicate experiments are observed. Most probably, there are two reasons for that: 1) the impact and friction of the mechanical stirrer on the films and the whole cell, leading to a random distraction of the layered structure from sample to sample, and 2) difficulties in precisely controlling the manufacturing of the cells. Regarding the latter, there are for example many features that can affect the kinetics of the dissolution reaction of Ag from cell to cell. One of them is the considerable range of the size of the Ag particles [41], as shown in Fig. 2b. Another two reasons are shown in Fig. 9, where the Ag grid lines (a and b) of an unleached sample are presented. It can easily be seen that the shape and thickness of the two lines differ. Also, in Fig. 9c one area with a high loss of surface area can be detected. The study of the Ag grid with SEM reveals many inhomogeneities, which can justify the high errors in the leaching kinetics of Ag. Regarding the rest of the layers, it is not possible to observe each one of them with SEM. However, according to the manufacturer, there are two reasons that can be responsible for the high errors in the leaching kinetics and also the total amounts: first, differences in the thickness of the layers from area to area (especially from the center to the edge) and, second, differences in grain sizes. According to the manufacturer, the thickest area has about double the thickness of the thinner, however, because of the totally symmetrical

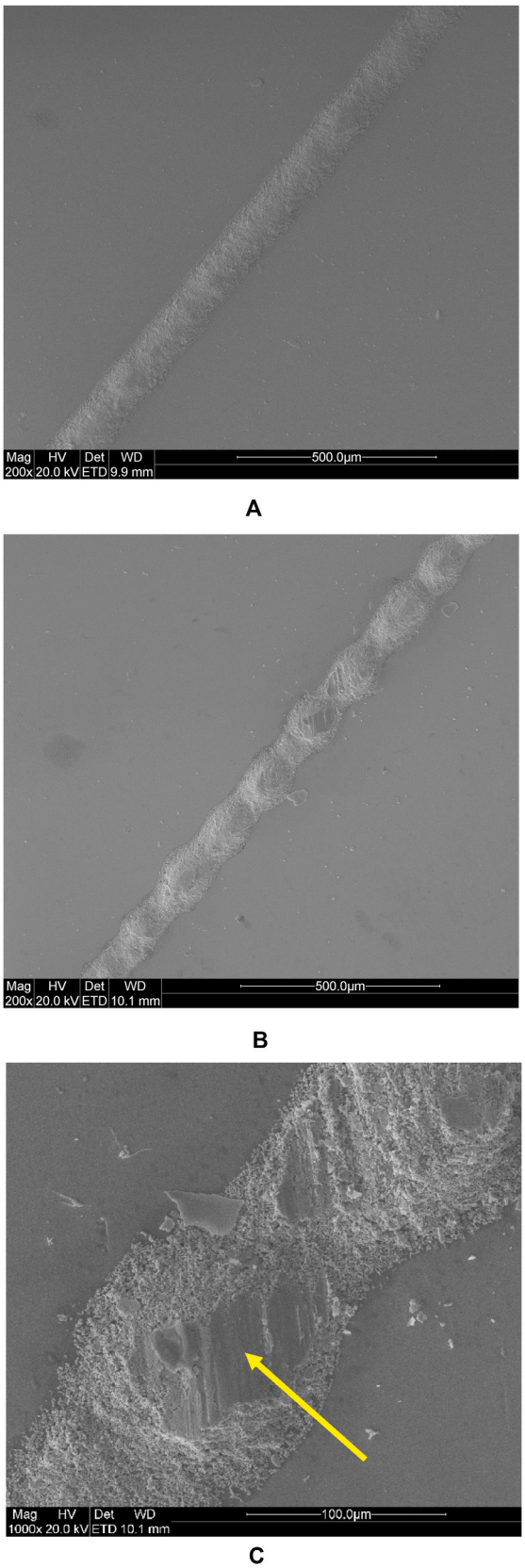

Fig. 9. SEM images of original CIGS cell taken with secondary electrons. a) and b) two different Ag grid lines and c) an area of the Ag grid line with considerable loss of surface area (see arrow).

way of cutting the cell into samples for the experiments, these differences are expected to be similar for all the samples. The grain size difference can be the significant factor that affects the leaching behaviors. This kind of variation is considered unavoidable during the manufacturing process.

4. Conclusions

It has been shown that the leaching yields of the elements Ag, Cr, Cu, Fe, Ga, In, Mo, Se, Sn, Ti and W which are present in flexible CIGS solar cells with an Ag grid and stainless steel substrate increase with the concentration of nitric acid from 0.1 to 2 M at room temperature. At the same time, for HNO_3 concentrations of 0.5 and 2 M, an increase in the yields was observed for all the elements except W when A:L ratio increases from 1:7 to 1:3 cm^2/ml, probably due to higher in-mixing of air and oxygenation of the solutions with smaller volumes. The only exception was Zn, which was leached completely under all the tested conditions, proving that low acid concentrations like 0.1 M are promising for its selective leaching in less than 1 h, improving the purity of Ag and In. It has also been shown that selective leaching of a considerable amount of Mo is possible by leaching with 0.5 M nitric acid and A:L ratio of 1:3 cm^2/ml for 6 h, however, optimization is needed for minimizing further any simultaneous leaching of Ag. The optimum result, a 100% efficiency for Ag and 85% of In, was achieved when leaching with 2 M HNO_3 and A:L 1:3 cm^2/ml for 24 h. A successive 24 h leaching step under the same conditions gave limited benefits in increasing the leaching yield of indium. This research suggests that recovery of valuable elements from CIGS material within 24 h is feasible without using harsh leaching conditions of elevated acid concentrations and temperatures and that related risks and costs can be reduced. At the same time, purity can also be improved by selective leaching of the contaminants, using benign conditions. Further optimization of the method should be investigated to develop viable metal recovery process from CIGS solar cells.

CRediT authorship contribution statement

Ioanna Teknetzi: Writing – original draft, Visualization, Validation, Methodology, Investigation, Formal analysis. **Stellan Holgersson:** Writing – review & editing, Supervision. **Burçak Ebin:** Writing – review & editing, Supervision, Resources, Project administration, Methodology, Funding acquisition, Conceptualization.

Declaration of competing interest

The authors declare that they have no known competing financial interests or personal relationships that could have appeared to influence the work reported in this paper.

Data availability

Data will be made available on request.

Acknowledgements

This work was funded by the Swedish Energy Agency [49349−1] (without any involvement from their side in the conduction of research and preparation of article). The authors would also like to thank Midsummer AB for kindly providing the solar cell samples and information on their manufacturing challenges. Finally, the authors would like to acknowledge the Chalmers Materials Analysis Laboratory, CMAL, for providing their facilities and assistance with the SEM-EDS analysis.

Appendix A. Supplementary data

Supplementary data to this article can be found online at https://doi.org/10.1016/j.solmat.2022.112178.

References

[1] International Energy Agency, Solar PV. https://www.iea.org/reports/solar-pv, 2021. (Accessed 17 September 2022).
[2] Fraunhofer institute for solar energy systems, PHOTOVOLTAICS REPORT. https://www.ise.fraunhofer.de/content/dam/ise/de/documents/publications/studies/Photovoltaics-Report.pdf, 2022. (Accessed 17 September 2022).
[3] Y. Cao, C. Liu, J. Jiang, X. Zhu, J. Zhou, J. Ni, J. Zhang, J. Pang, M.H. Rummeli, W. Zhou, H. Liu, G. Cuniberti, Theoretical insight into high-efficiency triple-junction tandem solar cells via the band engineering of antimony chalcogenides, RRL Sol 5 (4) (2021), 2000800, https://doi.org/10.1002/solr.202000800.
[4] M. Yamaguchi, F. Dimroth, J.F. Geisz, N.J. Ekins-Daukes, Multi-junction solar cells paving the way for super high-efficiency, J. Appl. Phys. 129 (2021), 240901, https://doi.org/10.1063/5.0048653.
[5] D. Sica, O. Malandrino, S. Supino, M. Testa, M.-C. Lucchetti, Management of end-of-life photovoltaic panels as a step towards a circular economy, Renew. Sustain. Energy Rev. 82 (2018) 2934–2945, https://doi.org/10.1016/j.rser.2017.10.039.
[6] International Energy Agency, End-of-Life management of photovoltaic panels: trends in PV module recycling technologies. https://iea-pvps.org/wp-content/uploads/2020/01/End_of_Life_Management_of_Photovoltaic_Panels_Trends_in_PV_Module_Recycling_Technologies_by_task_12.pdf, 2018. (Accessed 26 October 2022).
[7] M. Jost, E. Köhnen, A. Al-Ashouri, T. Bertram, S. Tomsič, A. Magomedov, E. Kasparavicius, T. Kodalle, B. Lipovsek, V. Getautis, R. Schlatmann, C. A. Kaufmann, S. Albrecht, M. Topič, Perovskite/CIGS tandem solar cells: from certified 24.2% toward 30% and beyond, ACS Energy Lett. 7 (4) (2022) 1298–1307, https://doi.org/10.1021/acsenergylett.2c00274.
[8] R.W. Miles, G. Zoppi, I. Forbes, Inorganic photovoltaic cells, Mater, Today Off. 10 (11) (2007) 20–27, https://doi.org/10.1016/S1369-7021(07)70275-4.
[9] J. Ramanujam, U.P. Singh, Copper indium gallium selenide based solar cells – a review, Energy Environ. Sci. 10 (6) (2017) 1306–1319, https://doi.org/10.1039/C7EE00826K.
[10] European Commission, Communication from the commission to the EUROPEAN parliament, in: THE EUROPEAN ECONOMIC and SOCIAL COMMITTEE and the COMMITTEE of the REGIONS Critical Raw Materials Resilience: Charting a Path towards Greater Security and Sustainability, THE COUNCIL, 2020. https://eur-lex.europa.eu/legal-content/EN/TXT/?uri=CELEX:52020DC0474. (Accessed 20 June 2022).
[11] A.-M. Balsberg Påhlsson, Toxicity of heavy metals (Zn, Cu, Cd, Pb) to vascular plants, Water Air Soil Pollut. 47 (1989) 287–319, https://doi.org/10.1007/BF00279329.
[12] P. Nain, A. Kumar, Ecological and human health risk assessment of metals leached from end-of-life solar photovoltaics, Environ. Pollut. 267 (2020), 115393, https://doi.org/10.1016/j.envpol.2020.115393.
[13] I.U. Rehman, M. Ishaq, L. Ali, S. Khan, I. Ahmad, I.U. Din, H. Ullah, Enrichment, spatial distribution of potential ecological and human health risk assessment via toxic metals in soil and surface water ingestion in the vicinity of Sewakht mines, district Chitral, Northern Pakistan, Ecotoxicol, Environ. Saf. 154 (2018) 127–136, https://doi.org/10.1016/j.ecoenv.2018.02.033.
[14] A.M.K. Gustafsson, M.R. StJ. Foreman, C. Ekberg, Recycling of high purity selenium from CIGS solar cell waste materials, Waste Manage. (Tucson, Ariz.) 34 (10) (2014) 1775–1782, https://doi.org/10.1016/j.wasman.2013.12.021.
[15] A.M.K. Gustafsson, B.-M. Steenari, C. Ekberg, Evaluation of high-temperature chlorination as a process for separation of copper, indium and gallium from CIGS solar cell waste materials, Separ. Sci. Technol. 50 (1) (2015) 1–9, https://doi.org/10.1080/01496395.2014.949350.
[16] A.M.K. Gustafsson, B.-M. Steenari, C. Ekberg, Recycling of CIGS solar cell waste materials: separation of copper, indium, and gallium by high-temperature chlorination reaction with ammonium chloride, Separ. Sci. Technol. 50 (15) (2015) 2415–2425, https://doi.org/10.1080/01496395.2015.1053569.
[17] Y. Lv, P. Xing, B. Ma, B. Liu, C. Wang, Y. Zhang, W. Zhang, Separation and recovery of valuable elements from spent CIGS materials, ACS Sustain. Chem. Eng. 7 (24) (2019) 19816–19823, https://doi.org/10.1021/acssuschemeng.9b05121.
[18] D. Hu, B. Ma, X. Li, Y. Lv, Y. Chen, C. Wang, Innovative and sustainable separation and recovery of valuable metals in spent CIGS materials, J. Clean. Prod. 350 (2022), 131426, https://doi.org/10.1016/j.jclepro.2022.131426.
[19] B. Ma, X. Li, B. Liu, P. Xing, W. Zhang, C. Wang, Y. Chen, Effective separation and recovery of valuable components from CIGS chamber waste via controlled phase transformation and selective leaching, ACS Sustain. Chem. Eng. 8 (7) (2020) 3026–3037. https://pubs.acs.org/doi/10.1021/acssuschemeng.0c00138.
[20] H.-I. Hsiang, C.-Y. Chiang, W.-H. Hsu, W.-S. Chen, J.-E. Chang, Leaching and re-synthesis of CIGS nanocrystallites from spent CIGS targets, Adv. Powder Technol. 27 (3) (2016) 914–920, https://doi.org/10.1016/j.apt.2016.02.012.
[21] S. Gu, B. Fu, G. Dodbiba, T. Fujita, B. Fang, Promising approach for recycling of spent CIGS targets by combining electrochemical techniques with dehydration and distillation, ACS Sustain. Chem. Eng. 6 (5) (2018) 6950–6956. https://pubs.acs.org/doi/10.1021/acssuschemeng.8b00787.
[22] H. Cui, G. Heath, T. Remo, D. Ravikumar, T. Silverman, M. Deceglie, M. Kempe, J. Engel-Cox, Technoeconomic analysis of high-value, crystalline silicon photovoltaic module recycling processes, Sol. Energy Mater. Sol. Cells 238 (2022), 111592, https://doi.org/10.1016/j.solmat.2022.111592.
[23] F.-W. Liu, T.-M. Cheng, Y.-J. Chen, K.-C. Yueh, S.-Y. Tang, K. Wang, C.-L. Wu, H.-S. Tsai, Y.-J. Yu, C.-H. Lai, W.-S. Chen, Y.-L. Chueh, High-yield recycling and

recovery of copper, indium, and gallium from waste copper indium gallium selenide thin-film solar panels, Sol. Energy Mater. Sol. Cells 241 (2022), 111691, https://doi.org/10.1016/j.solmat.2022.111691.
[24] X. Wang, X. Tian, X. Chen, L. Ren, C. Geng, A review of end-of-life crystalline silicon solar photovoltaic panel recycling technology, Sol. Energy Mater. Sol. Cells 248 (2022), 111976, https://doi.org/10.1016/j.solmat.2022.111976.
[25] E. Klugmann-Radziemska, P. Ostrowski, K. Drabczyk, P. Panek, M. Szkodo, Experimental validation of crystalline silicon solar cells recycling by thermal and chemical methods, Sol. Energy Mater. Sol. Cells 94 (12) (2010) 2275–2282, https://doi.org/10.1016/j.solmat.2010.07.025.
[26] L. Frisson, K. Lieten, T. Bruton, K. Declercq, J. Szlufcik, H. de Moor, M. Goris, A. Benali, O. Aceves, Recent Improvements in Industrial PV Module Recycling, 16th European Photovoltaic Solar Energy Conference, 1-5, May 2000 (Glasgow, UK).
[27] E. Klugmann-Radziemska, P. Ostrowski, Chemical treatment of crystalline silicon solar cells as a method of recovering pure silicon from photovoltaic modules, Renew. Energy 35 (8) (2010) 1751–1759, https://doi.org/10.1016/j.renene.2009.11.031.
[28] A. Kuczyńska-Łażewska, E. Klugmann-Radziemska, Z. Sobczak, T. Klimczuk, Recovery of silver metallization from damaged silicon cells, Sol. Energy Mater. Sol. Cells 176 (2018) 190–195, https://doi.org/10.1016/j.solmat.2017.12.004.
[29] W. Palitzsch, Method for Concentrating Metals from Scrap Containing Metal, WO2014166484A1, patent, 2014.
[30] S. Kang, S. Yoo, J. Lee, B. Boo, H. Ryu, Experimental investigations for recycling of silicon and glass from waste photovoltaic modules, Renew. Energy 47 (2012) 152–159, https://doi.org/10.1016/j.renene.2012.04.030.
[31] T.-Y. Wang, J.-C. Hsiao, C.-H. Du, 2012, Recycling of Materials from Silicon Base Solar Cell Module, 38th IEEE Photovoltaic Specialists Conference, Austin, TX, USA, 2012, https://doi.org/10.1109/PVSC.2012.6318071, 002355-002358.
[32] W. Palitzsch, U. Loser, in: A New and Intelligent De-metalization Step of Broken Silicon Cells and Silicon Cell Production Waste in the Recycling Procedure of Crystalline SI Modules, 2011 37th IEEE Photovoltaic Specialists Conference, IEEE, Seattle, WA, USA, 2011, pp. 3269–3270, https://doi.org/10.1109/PVSC.2011.6186635.
[33] S. Nieland, U. Neuhaus, T. Pfaff, E. Rädlein, New Approaches for Component Recycling of Crystalline Solar Modules, IEEE, 2012, Electronics Goes Green 2012+, Berlin, Germany, 2012, pp. 1–5.
[34] W.J. Gilbert, Corrosion in specialized environments, in: S.D. Cramer, B. S. Covino Jr. (Eds.), ASM Handbook Volume 13C Corrosion: Environments and Industries, ASM International, USA, 2006, p. 254.
[35] E. McCafferty, Getting started on the basics, in: Introduction to Corrosion Science, Springer, USA, 2010, pp. 15–22.
[36] R. Bender, D. Féron, D. Mills, S. Ritter, R. Bäßler, D. Bettge, I. De Graeve, A. Dugstad, S. Grassini, T. Hack, M. Halama, E.-H. Han, T. Harder, G. Hinds, J. Kittel, R. Krieg, C. Leygraf, L. Martinelli, A. Mol, D. Neff, J.-O. Nilsson, I. Odnevall, S. Paterson, S. Paul, T. Prošek, M. Raupach, R.I. Revilla, F. Ropital, H. Schweigart, E. Szala, H. Terryn, J. Tidblad, S. Virtanen, P. Volovitch, D. Watkinson, M. Wilms, G. Winning, M. Zheludkevich, Corrosion challenges towards a sustainable society, Mater. Corros. 73 (2022) 1–22, https://doi.org/10.1002/maco.202213140.
[37] ThermoFisher SCIENTIFIC, Selenious acid SAFETY DATA SHEET. https://www.fishersci.com/store/msds?partNumber=AC198870500&productDescription=SELENIOUS+ACID%2C+98%25+50GR&vendorId=VN00032119&countryCode=US&language=en, 2021. (Accessed 27 October 2022).
[38] L.M. Ferris, Solubility of molybdic oxide and its hydrates in nitric acid, nitric acid-ferric nitrate, and nitric acid-uranyl nitrate solutions, J. Chem. Eng. Data 6 (4) (1961) 600–603, https://doi.org/10.1021/je60011a035.
[39] The British Stainless Steel Association, Passivation of stainless steels. https://bssa.org.uk/bssa_articles/passivation-of-stainless-steels/ (accessed 10 July 2022).
[40] EDAX, Tips & tricks: Optimizing spatial resolution for EDS analysis. https://www.edax.com/-/media/ametekedax/files/resources/tips_tricks/optimizingspatialresolutionforedsanalysis.pdf (accessed 27 October 2022).
[41] J.-C. Lee, E.-Y. Kim, J.-H. Kim, W. Kim, B.-S. Kim, B.D. Pandey, Recycling of WC–Co hardmetal sludge by a new hydrometallurgical route, Int. J. Refract. Hard Met. 29 (3) (2011) 365–371, https://doi.org/10.1016/j.ijrmhm.2011.01.003.
[42] F. Faraji, A. Alizadeh, F. Rashchi N. Mostouf, Kinetics of leaching: a review, Rev. Chem. Eng. 38 (2) (2020) 113–148, https://doi.org/10.1515/revce-2019-0073.
[43] D.D. Ebbing, S.D. Gammon, Electrochemistry, in: General Chemistry, ninth ed., Houghton Mifflin Company, USA, 2009, pp. 785–786.
[44] B. Huang, X. Li, Y. Pei, S. Li, X. Cao, R.C. Massé, G. Cao, Novel carbon-encapsulated porous SnO_2 anode for lithium-ion batteries with much improved cyclic stability, Small 12 (14) (2016) 1945–1955, https://doi.org/10.1002/smll.201503419.
[45] S. Virolainen, D. Ibana, E. Paatero, Recovery of indium from indium tin oxide by solvent extraction, 1-2, Hydrometallurgy 107 (2011) 56–61, https://doi.org/10.1016/j.hydromet.2011.01.005.
[46] J. Schuster, B. Ebin, Investigation of indium and other valuable metals leaching from unground waste LCD screens by organic and inorganic acid leaching, Separ. Purif. Technol. 279 (2021), 119659, https://doi.org/10.1016/j.seppur.2021.119659.
[47] W.-H. Huang, W.J. Shin, L. Wang, M. Tao, Recovery of valuable and toxic metals from crystalline-Si modules, 2016, in: IEEE 43rd Photovoltaic Specialists Conference (PVSC), IEEE, Portland, OR, USA, 2016, pp. 3602–3605, https://doi.org/10.1109/PVSC.2016.7750344.